frontiers | Frontiers in Materials

TYPE Original Research
PUBLISHED 17 August 2023
DOI 10.3389/fmats.2023.1253090

OPEN ACCESS

EDITED BY
Noor Saeed Khan,
University of Education Lahore, Pakistan

REVIEWED BY
Ali Zabihi,
Rowan University, United States
Asad Ullah,
University of Lakki Marwat, Pakistan

*CORRESPONDENCE
Ahmed M. Hassan,
ahmed.hassan.res@fue.edu.eg

RECEIVED 04 July 2023
ACCEPTED 04 August 2023
PUBLISHED 17 August 2023

CITATION
Nagaraja KV, Vinutha K, Madhukesh JK, Khan U, Singh Chohan J, Sherif E-SM, Sarris IE, Hassan AM and Shanker B (2023), Thermal conductivity performance in sodium alginate-based Casson nanofluid flow by a curved Riga surface.
Front. Mater. 10:1253090.
doi: 10.3389/fmats.2023.1253090

Thermal conductivity performance in sodium alginate-based Casson nanofluid flow by a curved Riga surface

K. V. Nagaraja[1], K. Vinutha[2], J. K. Madhukesh[1], Umair Khan[3,4,5], Jasgurpreet Singh Chohan[6], El-Sayed M. Sherif[7], Ioannis E. Sarris[8], Ahmed M. Hassan[9]* and B. Shanker[10]

[1]Department of Mathematics, Amrita School of Engineering, Amrita Vishwa Vidyapeetham, Bengaluru, India, [2]Department of Studies in Mathematics, Davangere University, Davangere, India, [3]Department of Mathematical Sciences, Faculty of Science and Technology, Universiti Kebangsaan Malaysia, Bangi, Selangor, Malaysia, [4]Department of Computer Science and Mathematics, Lebanese American University, Byblos, Lebanon, [5]Department of Mathematics and Social Sciences, Sukkur IBA University, Sukkur, Sindh, Pakistan, [6]Department of Mechanical Engineering and University Centre for Research and Development, Chandigarh University, Mohali, Punjab, India, [7]Mechanical Engineering Department, College of Engineering, King Saud University, Riyadh, Saudi Arabia, [8]Department of Mechanical Engineering, University of West Attica, Athens, Greece, [9]Mechanical Engineering, Future University in Egypt, New Cairo, Egypt, [10]Department of Mathematics, CVR College of Engineering, Rangareddy, India

This study examines the effects of a porous media and thermal radiation on Casson-based nano liquid movement over a curved extending surface. The governing equations are simplified into a system of ODEs (ordinary differential equations) using the appropriate similarity variables. The numerical outcomes are obtained using the shooting method and Runge-Kutta Fehlbergs fourth-fifth order (RKF-45). An analysis is conducted to discuss the impact of significant nondimensional constraints on the thermal and velocity profiles. The findings show that the rise in curvature constraint will improve the velocity but diminish the temperature. The increased values of the modified Hartmann number raise the velocity, but a reverse trend is seen for increased porosity parameter values. Thermal radiation raises the temperature, while modified Hartmann numbers and the Casson factor lower the velocity but raise the thermal profile. Moreover, the existence of porous and solid fractions minimizes the surface drag force, and radiation and solid fraction components enhance the rate of thermal dispersion. The findings of this research may have potential applications in the design of heat exchangers used in cooling electronic devices like CPUs and GPUs, as well as microscale engines such as microturbines and micro-heat engines.

KEYWORDS

curved stretching sheet, Riga plate, casson nanofluid, thermal radiation, porous medium

1 Introduction

Fluid flow past a curved stretching sheet (CSS) is a classical fluid mechanics problem with numerous applications in engineering and physics. Investigating nanofluid flow over curved stretched sheets has become an attractive field of study due to its many useful applications, such as cooling in electronic devices, heat exchangers, processing of materials, solar collectors, synthesis of polymers, and microelectronic devices. The behavior of the fluid in this scenario depends on several factors, including the geometry of the surface, the velocity

of the stretching motion, and the properties of the fluid itself. Madhukesh et al. (Madhukesh et al., 2021) investigated the Newtonian heating (NH) and non-Fourier heat flux (NFHF) effect on the CSS in the presence of HNF (hybrid nanofluid). Multiple slippages on hydro-magnetic dissipative fluid across a CSS were addressed by Aihem et al. (Duraihem et al., 2023) and discussed their enhanced thermal and mass transmission properties. The impact of Cross dispersion on MHD Casson liquid movement along a CSS was inspected by Lakshmi et al. (Lakshmi et al., 2022). Sakkaravarthi et al. (Sakkaravarthi and Reddy, 2023) made a numerical investigation on entropy formation over a CHNF circulation over CSS. Simulation and theoretical inquiry on CNF over a CSS with the impact of a magnetic field and chemical processes were examined by Kumar et al. (Varun Kumar et al., 2022).

An electromagnetic actuator is a tool used in fluid mechanics to produce an effective liquid motion. A planar surface known as the Riga plate (RP) comprises alternating permanent magnets and electrodes. The magnetic field on the RP is not uniform, producing a Lorentz force that propels the fluid flow. In 1999, Gailitis and Lielausis (Gailitis and Lielausis, 1961) presented the electromagnetic actuator's basic theory for the first time. In contrast to typical techniques, they showed that employing electrodes and permanent magnets on a Riga plate may considerably increase the fluid flow rate and mixing capabilities. The advantage of employing an electromagnetic actuator to produce liquid flow is that it can do so without the need for mechanical actuators or movable components, which may be costly and prone to failure. Consequently, it is a viable solution for various practical purposes such as improving the exchange of heat, combining, and liquid flow. Asogwa et al. (Asogwa et al., 2022) examined analytical approaches to cross-diffusion and convection effects in the presence of CF over a porous RP. Hussain et al. (Hussain et al., 2022) investigated the impact of the Navier slip on an upward RP with CF displacement. Madhukesh et al. (Madhukesh et al., 2022a) investigated TPD and heat generation of Newtonian NF in an RP. Alshehri as al. (Mohammed Alshehri et al., 2021). Investigated Buoyancy implications in a Micropolar solution over an upward RP.

A nanofluid is a liquid with individual nanoparticles suspended in a solvent. Increased transfer of heat efficiency is a significant benefit of nanofluids over more traditional fluids. Increased thermal conductivity due to nanoparticles in the base fluid makes nanofluids excellent for thermal transfer medium. Nanofluids remain an intriguing field of study because of their revolutionary effects on a wide range of businesses and technology. The use of the change of variables approaches in the hydrothermal investigation of MHD compressing nanofluid circulation in parallel plates was studied by Zabihi et al. (Zabihi et al., 2022). Rizk et al. (Rizk et al., 2022) assessed the influence of the KKL correlation hypothesis on the production of thermal energies in a nanofluid comprising GO and ZnO dissolved in water passing via a permeable vertically spinning substrate. Shah et al. (Shah et al., 2021) researched mesoscopic modelling for magnetized nanofluid movement inside a porous three-dimensional tank. Ullah et al. (Ullah et al., 2022) scrutinized a magnetized 2D nanofluid that included blood, Go, and ZnO nanoparticles and moved via a perforated tube. The computational estimation of mixed convective entropy optimized in Darcy-Forchheimer circulation of Cross nanofluids via an upward plane plate with inconsistent heat source/sink was explored by Hussain et al. (Hussain et al., 2023).

When non-Newtonian behavior and nanofluids are combined, the result is a non-Newtonian nanofluid. Non-Newtonian fluids have a viscosity that varies as a function of the shear or stress rate. The temperature, nanoparticle concentration, and nanoparticle kind may impact this behavior. Khan et al. (Khan et al., 2023) investigated the effects of irregular heat source/sink on the aiding and opposing movements of the Eyring-Powell liquid on wall jet nanoparticles. Alharbi et al. (Alharbi et al., 2022) assessed the influence of viscous dissipation and Coriolis impacts on the mass and heat transmission evaluation of the 3D non-Newtonian flow of liquids. Khan et al. (Khan S. et al., 2021) investigated the study of the movement of a non-Newtonian liquid through a stretching/shrinking permeable material while considering the transmission of heat and mass. Some of the noticeable works on non-Newtonian fluids are found in (Algehyne et al., 2023; Alsulami et al., 2023).

The Casson nanofluid (CNF) idea is built on the assumption that the Casson equation governs liquid circulation and particle motion, a rheological model that explains the momentum behavior of non-Newtonian liquids. The Casson model considers yield stress and plastic solution viscosity, essential factors in various real-world scenarios such as blood circulation, coating layout, and liquid processing. Because of its improved thermal conductivity and specific heat capacity, CNF can considerably improve a fluid's ability to transmit temperature. Nanoparticles can also affect the fluid's rheological properties, such as viscosity and yield stress. Madhukesh et al. (Madhukesh et al., 2023) used the Cattaneo–Christov theory to investigate the heat transport of an MHD CMNF (Casson—Maxwell nanofluid) between two porous discs. Mabood et al. (Mabood et al., 2020) studied the free convective movement of time-dependent CNF in a permeable stretched surface. Madhukesh et al. (Madhukesh et al., 2022b) scrutinized the circulation of MHD MCNF in the presence of permeable discs using CCHF and slip impacts. Rasheed et al. (Rasheed et al., 2022) considered the homotopic solutions for the unsteady MHD CNF in a vertical cylinder with viscous dissipation impacts. The exact solution of a CF using Prabhakar-fractional simulations while also experiencing the effects of magnetohydrodynamic and sinusoidal thermal conditions was examined by Raza et al. (Raza et al., 2023).

Because of its temperature, a body emits a specific sort of electromagnetic radiation known as thermal radiation (TR). This radiation is formed by the thermal movement of the molecules and atoms inside the body, and it can go freely into space as there is no requirement for a medium to conduct it. The Stefan-Boltzmann equation describes the relationship between the temperature of a blackbody (an idealized object that absorbs all radiation incident on it) and the intensity of the thermal radiation it emits. Thermal radiation has important practical applications in various fields, including engineering, physics, astronomy, electronics, and energy conversion. Lone et al. (Lone et al., 2022) inspected MHD micropolar nanofluid hybrids circulating across a flat surface exposed to TR and mixed convection. Khan et al. (Khan U. et al., 2021) inspected the nonlinear T-R-influenced entropy production in the presence of NF with mixed convection effects. Naqvi et al. (Raza Shah Naqvi et al., 2022) examined numerical simulations to study the movement of hybrid nanofluids while considering the consequences of TR and entropy formation.

Ramesh et al. (Ramesh et al., 2023) scrutinized the hybrid-based CNT movement over a rotating sphere object in the presence of T-R and TPD. Magnetite-based liquid nanofluid three-dimensional layer movement involving non-linear TR and couple stress responses were studied by Ullah et al. (Ullah et al., 2021). The thermal study of slip and magnetohydrodynamic consequences for unstable sheet extending was investigated by Benos et al. (Benos et al., 2019).

The liquid and porous medium's features affect the rheological behavior of a fluid moving through them. When a non-Newtonian fluid, like a CNF, travels through a porous media, the pores' porosity, permeability, size, and shape can all impact how the fluid behaves. There has been a rise in interest in CNF flowing through porous media in recent years because of its potential applications in various industries, including increased oil recovery and geothermal energy generation. Understanding Casson nanofluid behavior is crucial for optimizing these processes since the characteristics of the porous medium can significantly impact how they behave. Alrehili et al. (Alrehili et al., 2022) made a numerical investigation of linear radiation and Soret impacts on MHD CNF over a vertical surface with a porous medium. Rallabandi et al. (Rallabandi, 2022) investigated the CNF flow over an inclined permeable stretched surface. Yogeesha et al. (Yogeesha et al., 2022) studied the Dufour and Soret effects to evaluate the dusty TNF circulation across an unstable stretched sheet. Raza et al. (Raza et al., 2022) inspected the activation energy, magnetic field, and binary chemical reaction impact on NF- and HNF through a porous area. Shoaib et al. (Shoaib et al., 2022) made soft computing to investigate the thermal energy's effects on the MHD CF as it passes over a porous material with an inclined non-linear surface.

The RKF-45, or Runge Kutta Fehlberg 4th 5th order, is a numerical method employed to solve complex systems of differential equations governing fluid flow problems. Many problems arise from simple laminar to complex turbulent flows in fluid mechanics. In mathematics, many of these situations may be modelled using ordinary differential equations, partial differential equations, or a hybrid of the two. Due to its high order accuracy and flexible step size capacity, RKF-45 is a popular numerical approach for modelling fluid dynamics. RKF-45 continuously controls the step size to reach the required level of precision while minimizing computational cost by calculating two estimates of the solution with varying orders of accuracy. The algorithm of the RKF-45 method is in detail given in (Mathews and Fink, 2004), and solving the differential equations using the RKF-45 algorithm was explained in (Abell and Braselton, 2000). Some works that implemented and used the RKF-45 algorithm are provided in (Sarris et al., 2002; Arifeen et al., 2021; Madhukesh et al., 2022b; Yogeesha et al., 2022; Hussain et al., 2023; Madhukesh et al., 2023).

The consider examination originality comes from its emphasis on the as-yet-unstudied subject of Casson-based nanofluid flow over a CSS in the presence of a porous medium and thermal radiation effects. In today's energy-conscious world, this study has the potential to help create more effective and sustainable thermal energy systems. Overall, studying the fluid flow past a CSS is an important area of research in fluid mechanics, with a significant impact on the development of microscale machines, including microfluidic devices, microscale engines, microsensors, and microscale reactors.

2 Mathematical formulation of the problem

As schematically seen in Figure 1, the flow pattern under study is a two-dimensional, incompressible, non-Newtonian Casson nanofluid flowing over a curved Riga surface. The radius of the curved surface is represented by R_1, and its curvilinear coordinates are marked by s_1& r_1. The uniform velocity of the Riga surface is $u_1 = U_{w1} = as_1$. Let T_{w1}& T_∞, respectively, stands for the wall and far-field temperatures. Suppose that the Riga surface is being affected by an electromagnetic force, denoted by F_m, in order to model the behavior of the fluid flow. A surface-mounted array of electrodes and permanent magnets are used to build the Riga surface. The previously derived governing equations for the fluid flow under these hypotheses are provided in the references (Hayat et al., 2018; Ahmad et al., 2019; Abbas et al., 2020; AdnanZaidi et al., 2020). These equations account for the influence of porous medium, TR, and CNF rheology on fluid flow across the curved Riga surface as follow:

$$R_1\frac{\partial u_1}{\partial s_1} + \frac{\partial}{\partial r_1}\left(v_1\left(R_1 + r_1\right)\right) = 0, \tag{1}$$

$$\frac{u_1^2}{\left(R_1 + r_1\right)} = \frac{1}{\rho_{nf}}\frac{\partial p_1}{\partial r_1}, \tag{2}$$

$$\begin{aligned}\frac{R_1}{\left(R_1 + r_1\right)}u_1\frac{\partial u_1}{\partial s_1} + v_1\frac{\partial u_1}{\partial r_1} + \frac{u_1 v_1}{\left(R_1 + r_1\right)} &= -\frac{1}{\rho_{nf}}\frac{R_1}{\left(R_1 + r_1\right)}\frac{\partial p_1}{\partial r_1} \\ &+ \exp\left(\frac{-\pi r_1}{c_1}\right)\frac{\pi j_0 M_0}{8\rho_{nf}} - \frac{\nu_{nf}}{k_1^*}u_1 + \nu_{nf}\left(1 + \frac{1}{\beta_1}\right) \\ &\left[\frac{\partial^2 u_1}{\partial r_1^2} + \frac{\partial u_1}{\partial r_1}\frac{1}{\left(R_1 + r_1\right)} - \frac{u_1}{\left(R_1 + r_1\right)^2}\right],\end{aligned} \tag{3}$$

$$\begin{aligned}\frac{R_1}{\left(R_1 + r_1\right)}u_1\frac{\partial T_1}{\partial s_1} + v_1\frac{\partial T_1}{\partial r_1} &= -\frac{k_{nf}}{\left(\rho C p\right)_{nf}}\left[\frac{\partial^2 T_1}{\partial r_1^2} + \frac{\partial T_1}{\partial r_1}\frac{1}{\left(R_1 + r_1\right)}\right] \\ &- \frac{1}{\left(\rho C p\right)_{nf}}\left[\frac{\partial}{\partial r_1}\left(\left(R_1 + r_1\right)q_r\right)\right]\frac{1}{\left(R_1 + r_1\right)}\end{aligned} \tag{4}$$

in Eq. 4, the term q_r is given by: $q_r = \frac{-16\sigma^* T_\infty^3}{3k^*}\frac{\partial T_1}{\partial r_1}$, [see (Hayat et al., 2018)].

The respective boundary conditions for the consider model are

$$\left.\begin{aligned} &r_1 = 0\text{: } u_1 = U_{w1}, v_1 = 0, T_1 = T_{w1}, \\ &r_1 \to \infty : u_1 \to 0, \frac{\partial u_1}{\partial r_1} \to 0, T_1 \to T_\infty. \end{aligned}\right\} \tag{5}$$

Furthermore, to ease the analysis of the consider investigation, the following similarity variables are introduced as [see (Abbas et al., 2020; AdnanZaidi et al., 2020)]:

$$\left.\begin{aligned} &\zeta = \left(\frac{U_1}{\nu_f s_1}\right)^{0.5} r_1, u_1 = U_1 h'(\zeta), v_1 = -\frac{R_1}{\left(R_1 + r_1\right)}\sqrt{\frac{U_1\nu_f}{s_1}}h(\zeta), \\ &p_1 = \rho_f {U_1}^2 P_1(\zeta), K_1 = \left(\frac{U_1}{\nu_f s_1}\right)^{0.5} R_1, \theta = \frac{T_1 - T_\infty}{T_{w1} - T_\infty}. \end{aligned}\right\} \tag{6}$$

Therefore, with the help of the above similarity variables stated in Eqs 1, 6 is satisfied and Eqs 2, 3 take the following form as:

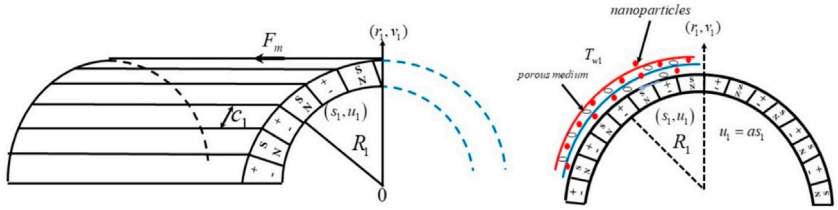

FIGURE 1
Geometry of the flow problem.

$$P_1' = \frac{h'^2 G_2}{\zeta + K_1}, \tag{7}$$

$$\frac{2K_1}{\zeta + K_1}\frac{P_1}{G_2} = \left(1 + \frac{1}{\beta_1}\right)\left[h''' + \frac{1}{\zeta + K_1}h'' - \frac{h'}{(\zeta + K_1)^2}\right]\frac{1}{G_1 G_2} + \frac{K_1}{\zeta + K_1}\left(hh'' - (h')^2\right) + \frac{K_1}{(\zeta + K_1)^2}h'h + \frac{Q_1 e^{-z\zeta}}{G_2} - \frac{\lambda_1}{G_1 G_2}h'. \tag{8}$$

here, $Q_1 = \frac{\pi j_0 M_0}{8\rho_f U_1 a}$ is the modified Hartmann number, $\lambda_1 = \frac{\nu_f}{k^*_1 a}$ is the porous parameter, and $z = \sqrt{\frac{\pi^2 \nu_f}{a c_1^2}}$ is the parameter related to the width of the magnets and electrodes.

Moreover, to eliminate the pressure terms in Eqs 7, 8, we get

$$\left(1 + \frac{1}{\beta_1}\right)\left[\frac{h'}{(\zeta + K_1)^3} - \frac{h''}{(\zeta + K_1)^2} + \frac{2}{\zeta + K_1}h''' + h''''\right]\frac{1}{G_1 G_2} + \frac{K_1}{\zeta + K_1}(hh''' - h'h'') + \frac{K_1}{(\zeta + K_1)^2}\left(hh'' - h'^2\right) - \frac{K_1}{(\zeta + K_1)^3}h'h + w_2\frac{Q_1 e^{-z\zeta}}{G_2} - \frac{\lambda_1}{G_1 G_2}\left(h'' + \frac{h'}{\zeta + K_1}\right) = 0. \tag{9}$$

After utilizing the similarity variables, the energy Eq. 4 reduces to the form as:

$$\left[\frac{k_{nf}}{k_f} + \frac{4}{3}Nr\right]\frac{1}{\mathrm{Pr}G_3}\left(\theta'' + \frac{1}{\zeta + K_1}\theta'\right) + \frac{K_1}{\zeta + K_1}h\theta' = 0, \tag{10}$$

with simplified boundary conditions are

$$\left.\begin{array}{l}\zeta = 0\text{: } h'(\zeta) = 1, h(\zeta) = 0, \theta(\zeta) = 1.\\ \zeta \to \infty : h'(\zeta) = 0, h''(\zeta) = 0, \theta(\zeta) = 0.\end{array}\right\} \tag{11}$$

in aforesaid Eqs 9–11, the term $w_2 = (\frac{1}{\zeta + K_1} - z)$ is called a dimensionless quantity, $\mathrm{Pr}\frac{\nu_f (\rho C p)_f}{k_f}$, & $Nr = \frac{4\phi^* T_\infty^3}{k^* k_f}$ refer the Prandtl number, and radiation parameter, respectively.

The important engineering quantities and its reduced form [see (Abbas et al., 2020; AdnanZaidi et al., 2020)]:

$$Cf = \frac{\mu_{nf}}{\rho_f U_{w1}^2}\left(1 + \frac{1}{\beta_1}\right)\left(\frac{\partial u_1}{\partial r_1} - \frac{u_1}{(R_1 + r_1)}\right)_{r_1 = 0} \Rightarrow \sqrt{\mathrm{Re}}Cf = \frac{1}{G_1}\left(1 + \frac{1}{\beta_1}\right)\left(h''(0) - \frac{h'(0)}{\zeta + K_1}\right), \tag{12}$$

$$Nu = \frac{-s_1}{k_f (T_{w1} - T_\infty)}\left(k_{nf} + \frac{16\phi^* T_\infty^3}{3k^*}\right)\left(\frac{\partial T_1}{\partial r_1}\right)_{r_1 = 0} \Rightarrow \frac{Nu}{\sqrt{\mathrm{Re}}} = \left[\frac{k_{nf}}{k_f} + \frac{4}{3}Nr\right]\theta'(0). \tag{13}$$

TABLE 1 Thermophysical properties of base fluid and nanoparticles.

Properties	$SA(C_6H_9NaO_7)$	TiO_2
$\rho(kgm^{-3})$	989	4250
$C_p(Jkg^{-1}K^{-1})$	4175	686.2
$k(kgms^{-3}K^{-1})$	0.6376	8.9528
Pr	6.45	-

TABLE 2 Comparison of $-Cf$ values of current numerical implementation with the work of (Sajid et al., 2010) in the absence of $G_1, G_2, (1 + \frac{1}{\beta_1})$ and $Q_1 = 0$.

Parameter	Sajid et al. (2010)	Present work
$K = 20$	0.9357	0.93588
$K = 30$	0.9568	0.95612
$K = 40$	0.9675	0.96787
$K = 50$	0.9740	0.97445
$K = 100$	0.9870	0.98797

Hence, $\mathrm{Re} = \frac{U_1 s_1}{\nu_f}$ is the local Reynolds number.

The thermophysical properties of nanofluid are given as follows [see (Khan et al., 2018; Alwawi et al., 2019)].

The effective thermophysical characteristics of nanofluid are given as follows [see (Acharya et al., 2019)]

$$\mu_{nf} = \frac{\mu_f}{G_1}\left(G_1 = (1 - \phi^*)^{2.5}\right), \tag{14}$$

$$\rho_{nf} = \rho_f G_2\left(G_2 = \left(1 - \phi^* + \frac{\phi^* \rho_s}{\rho_f}\right)\right), \tag{15}$$

$$(\rho C p)_{nf} = (\rho C p)_f G_3\left(G_3 = \left(1 - \phi^* + \frac{\phi^* \rho_s C p_s}{\rho_f C p_f}\right)\right), \tag{16}$$

$$\frac{k_{nf}}{k_f} = \frac{k_s - 2\phi^*\left(k_f - k_s\right) + 2k_f}{k_s + \phi^*\left(k_f - k_s\right) + 2k_f}. \tag{17}$$

3 Numerical method and code validation

The higher order and two-point boundary conditions in the governing equations for the fluid flow over the curved Riga

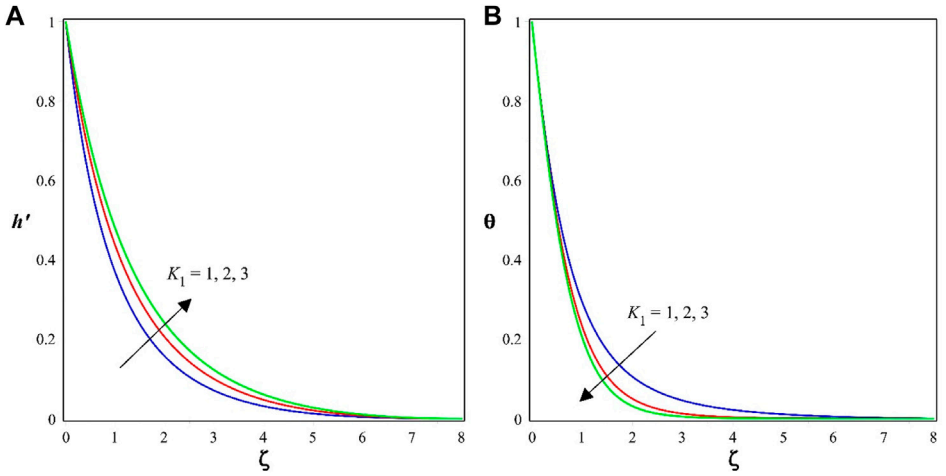

FIGURE 2
Significance of K_1 on **(A)** velocity profile **(B)** temperature profile.

surface make them challenging to solve analytically. We must transform these into first-order differential equations to achieve a numerical solution. Applying appropriate transformations will allow the higher-order differential equations to be represented as a set of first-order differential equations. Let us take,

$$\begin{matrix}[h, h', h'', h'''] = [\kappa_1, \kappa_2, \kappa_3, \kappa_4] \\ [\theta, \theta'] = [\kappa_5, \kappa_6]\end{matrix}, \tag{18}$$

$$h'''' = \frac{-G_1G_2}{\left(1+\frac{1}{\beta_1}\right)}\left(\begin{array}{l}\left(1+\frac{1}{\beta_1}\right)\frac{1}{G_1G_2}\left(\frac{2}{\zeta+K_1}\kappa_4 - \frac{\kappa_3}{(\zeta+K_1)^2}+\frac{\kappa_2}{(\zeta+K_1)^3}\right) \\ +\frac{K_1}{\zeta+K_1}(\kappa_1\kappa_4-\kappa_2\kappa_3)+\frac{K_1}{(\zeta+K_1)^2}(\kappa_1\kappa_3-\kappa_2{}^2) \\ -\frac{K_1}{(\zeta+K_1)^3}\kappa_2\kappa_1+w_2\frac{Q_1e^{-z\zeta}}{G_2}-\frac{\lambda_1}{G_1G_2}\left(\kappa_3+\frac{\kappa_2}{\zeta+K_1}\right)\end{array}\right), \tag{19}$$

$$\theta'' = -\frac{\mathrm{PrG_3}}{\left[\frac{k_{nf}}{k_f}+\frac{4}{3}Nr\right]}\left(\frac{K_1}{\zeta+K_1}\kappa_1\kappa_6+\frac{1}{\zeta+K_1}\kappa_6\frac{1}{\mathrm{PrG_3}}\left[\frac{k_{nf}}{k_f}+\frac{4}{3}Nr\right]\right), \tag{20}$$

with the boundary constraints become

$$\left.\begin{matrix}\kappa_1(0)=0, \kappa_2(0)=1, \kappa_3(0)=\chi_1, \kappa_4(0)=\chi_2, \\ \kappa_5(0)=1, \kappa_4(0)=\chi_3.\end{matrix}\right\} \tag{21}$$

The Runge-Kutta Fehlberg 45-order approach was then used to solve the transformed Eq. 19 numerically and (20) as well as the boundary conditions (21). Since the boundary conditions contain unknowns, we employed a shooting technique to find the solution that meets the conditions at infinity. Further, utilised a step size of 0.001 and set the error tolerance to 10^{-6} to achieve accurate findings. By substituting appropriate values for the dimensionless variables and using the thermophysical properties of the nanofluid (see Table 1) solutions are obtained. We discovered that our findings were in strong accord with prior work (Sajid et al., 2010), demonstrating the accuracy and dependability of our numerical method (see Table 2).

4 Results and discussion

The purpose of this section is to describe how significant dimensionless parameters affect the temperature and velocity profiles. The RKF-45 method and shooting approach are used to numerically solve the reduced ODEs and boundary conditions acquired in the previous section. The acquired data are shown as graphs to illustrate the impact of various dimensionless parameters on the motion and temperature fields. Also, a discussion of the important technical variables that may have an impact on the system's flow and thermal transfer characteristics is included in this section. The current study offers useful insights for designing and optimising industrial applications employing Casson-based nanofluid movements over curved surfaces by taking these parameters into account.

Figures 2A, B show the impact of K_1 (curvature constraint) over velocity and temperature profiles, respectively. According to the findings, a rise in the curvature parameter improves the h' profile (Figure 2A) but lowers the θ profile (Figure 2B). This is explained by the fact that increasing the radius of the curved surface causes the fluid to move more quickly, which improves the velocity profile by reducing the thickness of both the momentum boundary layer (MBL) and thermal boundary layer (TBL). However, when the fluid moves more quickly, there is less time for temperature distribution, which reduces temperature.

Figure 3A, B display the variation of h' and θ profiles in the presence of Q_1 (modified Hartmann number). The improvement in the Q_1 will decreases the velocity profile (see Figure 3A) but improves the temperature profile (see Figure 3B). This is caused by a rise in the Q_1, which slows the liquid flow and lowers the velocity profile by increasing the magnetic strength and, consequently, the Lorentz force. Yet, this also improves the system's thermal distribution, leading to a better temperature profile.

The effect of the porosity constraint λ_1 on the h' profile is illustrated in Figure 4A. It has been found that a higher λ_1 causes the velocity profile to drop. This is due to the presence of a porous

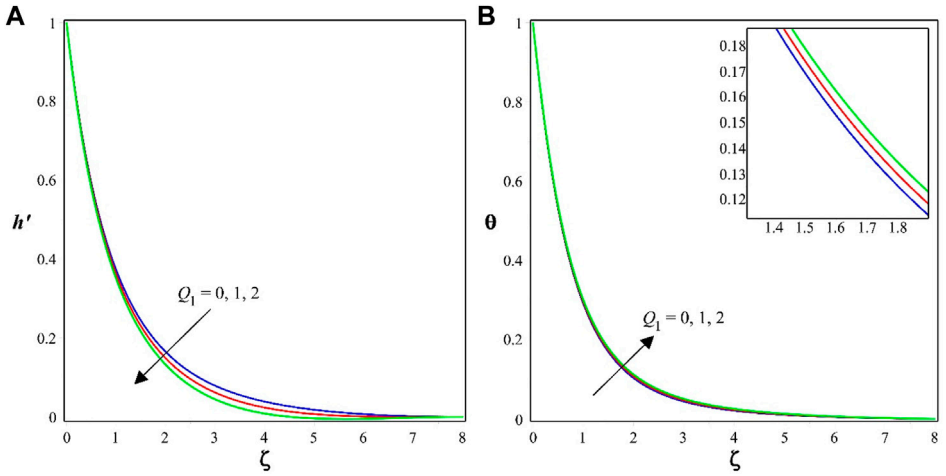

FIGURE 3
Significance of Q_1 on **(A)** velocity profile **(B)** temperature profile.

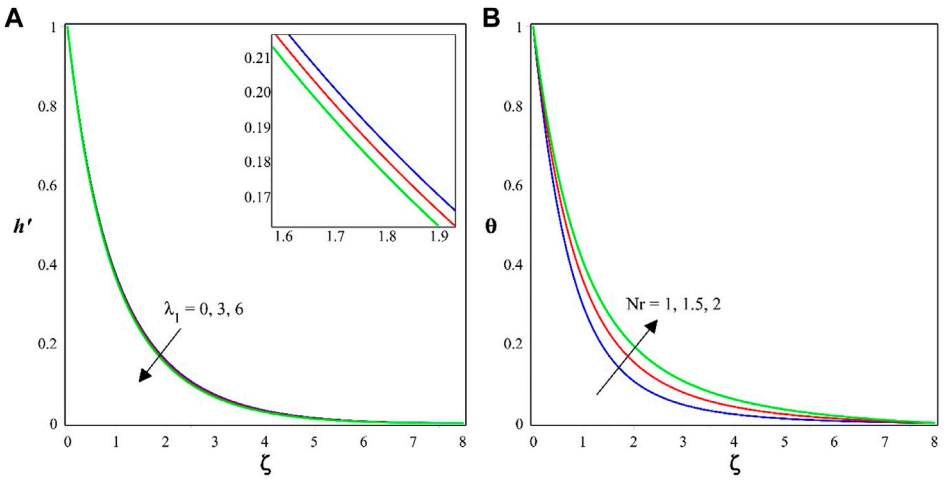

FIGURE 4
(A) Significance of λ_1 on velocity profile **(B)** Significance of *Nr* on temperature profile.

medium, which restricts the movement of fluids by providing a barrier against the motion of the fluids. The h' profile is decreased when the resistance rises along with the porous parameter. Figure 4B displayed the influence of the thermal radiation Nr parameter on θ profile. The rise in Nr will improve the temperature profile. An increase in the value of Nr denotes a rise in the system's thermal radiation output. The energy from the radiation is absorbed by the fluid, raising its temperature, which improves the temperature profile.

The consequence of the Casson parameter β_1 on the h' profile is represented in Figure 5A. It is evident that a rise in the values of β_1 causes the velocity profile to fall. This is because a greater β_1 causes the fluid's yield stress to flow initiation and decrease the h' profile. This leads to decline in the overall velocity of the liquid near the boundary as the circulation is impeded by increasing yield stress. Figure 5B displays the variation of θ profile for numerous values of the Casson parameter β_1. The rise in the values of β_1 will advance the temperature distribution. As explained in Figure 5A, the reduction in the velocity will lead to the liquid's residence time near the surface. When the β_1 increases, it implies a larger yield stress, meaning that the liquid requires more energy to commence flow. As a result of the higher flow resistance, more energy is released as heat inside the fluid. The temperature profile rises as a result of this phenomena.

Figure 6A represents the effect of skin friction on the porous parameter λ_1 for the rise in the values of solid volume fraction ϕ^*. It is observed that surface drag force decreases with improved values of λ_1 and ϕ^*. This is due to the fact that raising these parameters generates an increase in the MBL's thickness, which in turn causes a reduction in the fluid flow at the surface. As a direct consequence of this, the force of surface drag is decreased. Figure 6B shows the variation in Nusselt number for improved values of Nr and ϕ^*.

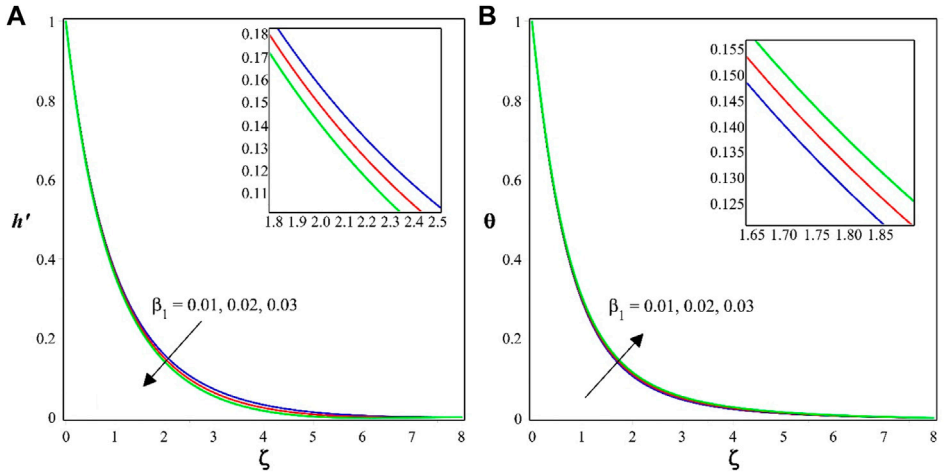

FIGURE 5
Significance of β_1 on **(A)** velocity profile **(B)** temperature profile.

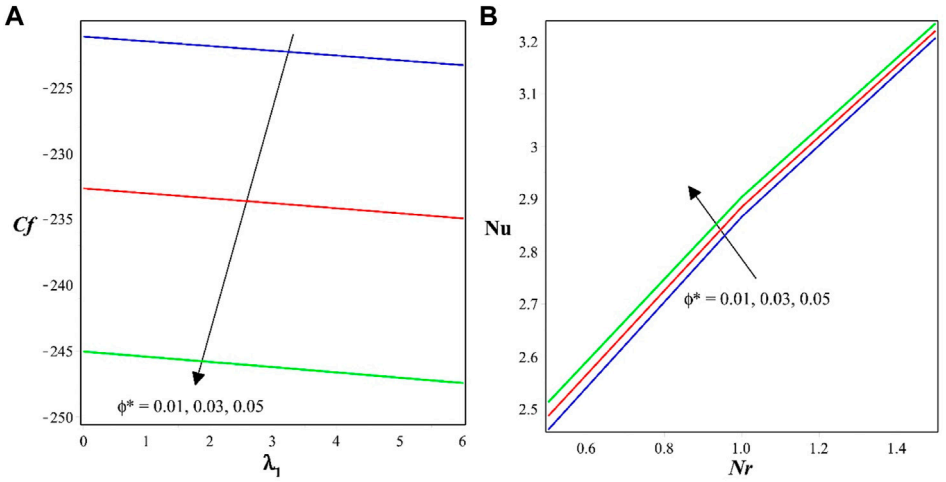

FIGURE 6
(A) Impact of *Cf* on λ_1 for different values of ϕ^* **(B)** Impact of *Cf* on *Nr* for different values of ϕ^*.

When these two criteria are improved, the rate at which thermal energy is distributed will increase. However, because nanoparticles are present in the fluid, the thermal conductivity is boosted, which results in an increase in the total heat transfer rate. This offsets the fact that the surface area that is accessible for heat transmission decreases as the percentage rises.

5 Final remarks

The present study investigates Casson-based nanofluid movement over a curved stretching surface in the presence of porous medium and thermal radiation effects. The ODEs and BCs are obtained by applying suitable similarity constraints to the PDEs. The numerical calculations are done with the aid of RKF-45 and shooting techniques. The outcomes are visualized using a graphical representation. The discussions on important dimensionless constraints are presented. The main conclusions of the study are as follows:

- ❖ The improvement in the modified Hartman number and porosity factors will decrease the velocity. An increase in these components indicates stronger magnetic impacts and increased permeability. As a result, the velocity of the flow of nanofluid reduces.
- ❖ With an increase in the curvature parameter, the velocity rises but the temperature decreases. The surface becomes increasingly curved when the curvature parameter is increased. This causes higher liquid flow along the curved surface, which causes velocity to go up. The temperature, on the other hand, falls as the liquid moves more and releases heat owing to the increasing surface area.

- ❖ Thermal radiation and modified Hartmann numbers will improve the temperature. Thermal radiation and modified Hartmann numbers facilitates the distribution of heat from liquid to the surrounding and improves the thermal distribution due to strong magnetic effects.
- ❖ The Casson factor will decline the velocity but improve the thermal profile. The rise in Casson factor will denotes the higher yield stress and more resistance to flow of the liquid. This results in decrease in velocity and improved thermal profile.
- ❖ The surface drag force reduces with increase in the values of porous and solid fractions. Porous medium act as a barrier and slows down the fluid flow and adding of solid particles also influence on the surface drag force by increasing thickness of momentum boundary layer.
- ❖ The rate of thermal distribution advances with radiation and solid fraction factors. Heat transport is facilitated by radiation, and the thermal distribution is improved by the presence of solid fractions, which encourage better mixing and dispersion of thermal energy.

Data availability statement

The original contributions presented in the study are included in the article/Supplementary Material, further inquiries can be directed to the corresponding author.

Author contributions

Conceptualization, AH, BS, KN, KV, and JM; methodology, KN, KV, and JM; software, KN, KV, and JM; validation, KN, KV, and JM; formal analysis, KN, KV, and JM; investigation, UK, JS, and IS; resources, IS; data curation, AH, BS, UK, JS, and IS; writing—original draft preparation, AH, BS, UK, JS, IS, and E-SS; writing—review and editing, AH, BS, UK, JS, IS, and E-SS; visualization, E-SS; supervision, E-SS; project administration, E-SS; funding acquisition, E-SS. All authors contributed to the article and approved the submitted version.

Funding

This work was funded by the Researchers Supporting Project number (RSP2023R33), King Saud University, Riyadh, Saudi Arabia.

Acknowledgments

The authors are thankful for the support of Researchers Supporting Project number (RSP2023R33), King Saud University, Riyadh, Saudi Arabia.

Conflict of interest

The authors declare that the research was conducted in the absence of any commercial or financial relationships that could be construed as a potential conflict of interest.

Publisher's note

References

Abbas, N., Malik, M. Y., and Nadeem, S. (2020). Transportation of magnetized micropolar hybrid nanomaterial fluid flow over a Riga curface surface. *Comput. Methods Programs Biomed.* 185, 105136. doi:10.1016/j.cmpb.2019.105136

Abell, M. L., and Braselton, J. P. (2000). *Differential equations with maple V*. Cambridge, Massachusetts, United States: Academic Press.

Acharya, N., Maity, S., and Kundu, P. K. (2019). Framing the hydrothermal features of magnetized TiO2–CoFe2O4 water-based steady hybrid nanofluid flow over a radiative revolving disk. *Multidiscip. Model. Mater. Struct.* 16, 765–790. doi:10.1108/mmms-08-2019-0151

AdnanZaidi, S. Z. A., Khan, U. N., Chu, Y. M., Mohyud-Din, S. T., Chu, Y.-M., Khan, I. K. S., et al. (2020). Impacts of freezing temperature based thermal conductivity on the heat transfer gradient in nanofluids: applications for a curved Riga surface. *Molecules* 25, 2152. doi:10.3390/molecules25092152

Ahmad, S., Nadeem, S., and Muhammad, N. (2019). Boundary layer flow over a curved surface imbedded in porous medium. *Commun. Theor. Phys.* 71, 344. doi:10.1088/0253-6102/71/3/344

Algehyne, E. A., Abdelmohsen, S. A. M., Gowda, R. J. P., Kumar, R. N., Abdelbacki, A. M. M., Gorji, M. R., et al. (2023). Mathematical modeling of magnetic dipole effect on convective heat transfer in Maxwell nanofluid flow: single and multi-walled carbon nanotubes. *Waves Random Complex Media* 33, 489–504. doi:10.1080/17455030.2022.2125598

Alharbi, K. A. M., Ullah, A., Ikramullah, Fatima, N., Khan, R., Sohail, M., et al. (2022). Impact of viscous dissipation and coriolis effects in heat and mass transfer analysis of the 3D non-Newtonian fluid flow. *Case Stud. Therm. Eng.* 37, 102289. doi:10.1016/j.csite.2022.102289

Alrehili, M. F., Goud, B. S., Reddy, Y. D., Mishra, S. R., Lashin, M. M. A., Govindan, V., et al. (2022). Numerical computing of Soret and linear radiative effects on MHD Casson fluid flow toward a vertical surface through a porous medium: finite element analysis. *Mod. Phys. Lett. B* 36, 2250170. doi:10.1142/s0217984922501706

Alsulami, M. D., Naveen Kumar, R., Punith Gowda, R. J., and Prasannakumara, B. C. (2023). Analysis of heat transfer using Local thermal non-equilibrium conditions for a non-Newtonian fluid flow containing Ti6Al4V and AA7075 nanoparticles in a porous media. *ZAMM - J. Appl. Math. Mech./ Zeitschrift Für Angewandte Math. Und Mech.* 103, e202100360. doi:10.1002/zamm.202100360

Alwawi, F. A., Alkasasbeh, H. T., Rashad, A. M., and Idris, R. (2019). Natural convection flow of Sodium Alginate based Casson nanofluid about a solid sphere in the presence of a magnetic field with constant surface heat flux. *J. Phys. Conf. Ser.* 1366, 012005. doi:10.1088/1742-6596/1366/1/012005

Arifeen, S. U., Haq, S., Ghafoor, A., Ullah, A., Kumam, P., and Chaipanya, P. (2021). Numerical solutions of higher order boundary value problems via wavelet approach. *Adv. Differ. Equ.* 2021, 347. doi:10.1186/s13662-021-03495-6

Asogwa, K. K., Alsulami, M. D., Prasannakumara, B. C., and Muhammad, T. (2022). Double diffusive convection and cross diffusion effects on Casson fluid over a Lorentz force driven Riga plate in a porous medium with heat sink: an analytical approach. *Int. Commun. Heat Mass Transf.* 131, 105761. doi:10.1016/j.icheatmasstransfer.2021.105761

Benos, L. Th., Mahabaleshwar, U. S., Sakanaka, P. H., and Sarris, I. E. (2019). Thermal analysis of the unsteady sheet stretching subject to slip and magnetohydrodynamic effects. *Therm. Sci. Eng. Prog.* 13, 100367. doi:10.1016/j.tsep.2019.100367

Duraihem, F. Z., Devi, R. L. V. R., Prakash, P., Sreelakshmi, T. K., Saleem, S., Durgaprasad, P., et al. (2023). Enhanced heat and mass transfer characteristics of multiple slips on hydro-magnetic dissipative Casson fluid over a curved stretching surface. *Int. J. Mod. Phys. B*, 2350229. doi:10.1142/s0217979223502296

Gailitis, A., and Lielausis, O. (1961). On a possibility to reduce the hydrodynamic resistance of a plate in aelectro-lyte. *Appl. Magnetohydrodyn.* 12, 143–146.

Hayat, T., Qayyum, S., Imtiaz, M., and Alsaedi, A. (2018). Double stratification in flow by curved stretching sheet with thermal radiation and joule heating. *J. Therm. Sci. Eng. Appl.* 10, 021010. doi:10.1115/1.4037774

Hussain, S. M., Khan, U., Zaib, A., Ishak, A., and Sarris, I. E. (2023). Numerical computation of mixed convective entropy optimized in Darcy-Forchheimer flow of Cross nanofluids through a vertical flat plate with irregular heat source/sink. *Tribol. Int.* 187, 108757. doi:10.1016/j.triboint.2023.108757

Hussain, S. M., Sharma, R., and Alrashidy, S. S. (2022). Numerical study of Casson nanofluid flow past a vertical convectively heated Riga-plate with Navier's slip condition. *AIP Conf. Proc.* 2435, 020002. doi:10.1063/5.0083603

Khan, A., Khan, D., Khan, I., Ali, F., ul Karim, F., and Imran, M. (2018). MHD flow of sodium alginate-based casson type nanofluid passing through A porous medium with Newtonian heating. *Sci. Rep.* 8, 8645. doi:10.1038/s41598-018-26994-1

Khan, S., Selim, M. M., Khan, A., Ullah, A., Abdeljawad, T., Ikramullah,, et al. (2021a). On the analysis of the non-Newtonian fluid flow past a stretching/shrinking permeable surface with heat and mass transfer. *Coatings* 11, 566. doi:10.3390/coatings11050566

Khan, U., Zaib, A., Ishak, A., Sherif, E.-S. M., Sarris, I. E., Eldin, S. M., et al. (2023). Analysis of assisting and opposing flows of the Eyring-Powell fluid on the wall jet nanoparticles with significant impacts of irregular heat source/sink. *Case Stud. Therm. Eng.* 49, 103209. doi:10.1016/j.csite.2023.103209

Khan, U., Zaib, A., Khan, I., and Nisar, K. S. (2021b). Entropy generation incorporating γ-nanofluids under the influence of nonlinear radiation with mixed convection. *Crystals* 11, 400. doi:10.3390/cryst11040400

Lakshmi, K. B., Sugunamma, V., Tarakaramu, N., Sivakumar, N., and Sivajothi, R. (2022). Cross-dispersion effect on magnetohydrodynamic dissipative Casson fluid flow via curved sheet. *Heat. Transf.* 51, 7822–7842. doi:10.1002/htj.22668

Lone, S. A., Alyami, M. A., Saeed, A., Dawar, A., Kumam, P., and Kumam, W. (2022). MHD micropolar hybrid nanofluid flow over a flat surface subject to mixed convection and thermal radiation. *Sci. Rep.* 12, 17283. doi:10.1038/s41598-022-21255-8

Mabood, F., Yusuf, T. A., and Sarris, I. E. (2020). Entropy generation and irreversibility analysis on free convective unsteady mhd casson fluid flow over a stretching sheet with soret/dufour in porous media. *STRPM* 11, 595–611. doi:10.1615/specialtopicsrevporousmedia.2020033867

Madhukesh, J. K., Naveen Kumar, R., Punith Gowda, R. J., Prasannakumara, B. C., Ramesh, G. K., Ijaz Khan, M., et al. (2021). Numerical simulation of aa7072-aa7075/water-based hybrid nanofluid flow over a curved stretching sheet with Newtonian heating: a non-fourier heat flux model approach. *J. Mol. Liq.* 335, 116103. doi:10.1016/j.molliq.2021.116103

Madhukesh, J. K., Prasannakumara, B. C., Kumar, R. S. V., Rauf, A., and Shehzad, S. A. (2022b). Flow of hydromagnetic micropolar-casson nanofluid over porous disks influenced by cattaneo-christov theory and slip effects. *JPM* 25, 35–49. doi:10.1615/jpormedia.2021039254

Madhukesh, J. K., Ramesh, G. K., Shehzad, S. A., Chapi, S., and Prabhu Kushalappa, I. (2023). Thermal transport of MHD Casson–Maxwell nanofluid between two porous disks with Cattaneo–Christov theory. *Numer. Heat. Transf. Part A Appl.*, 1–16. doi:10.1080/10407782.2023.2214322

Madhukesh, J. K., Varun Kumar, R. S., Punith Gowda, R. J., Prasannakumara, B. C., and Shehzad, S. A. (2022a). Thermophoretic particle deposition and heat generation analysis of Newtonian nanofluid flow through magnetized Riga plate. *Heat. Transf.* 51, 3082–3098. doi:10.1002/htj.22438

Mathews, J. H., and Fink, K. D. (2004). *Numerical methods using MATLAB*. Upper Saddle River, NJ, USA: Pearson Prentice Hall.

Mohammed Alshehri, A., Huseyin Coban, H., Ahmad, S., Khan, U., and Alghamdi, W. M. (2021). Buoyancy effect on a micropolar fluid flow past a vertical Riga surface comprising water-based SWCNT–MWCNT hybrid nanofluid subject to partially slipped and thermal stratification: cattaneo–christov model. *Math. Problems Eng.* 2021, 1–13. doi:10.1155/2021/6618395

Rallabandi, S. R. (2022). Finite element solutions of non-Newtonian dissipative Casson fluid flow past a vertically inclined surface surrounded by porous medium including constant heat flux, thermal diffusion, and diffusion thermo. *Int. J. Comput. Methods Eng. Sci. Mech.* 23, 228–242. doi:10.1080/15502287.2021.1949407

Ramesh, G. K., Madhukesh, J. K., Ali Shah, N., and Yook, S.-J. (2023). Flow of hybrid CNTs past a rotating sphere subjected to thermal radiation and thermophoretic particle deposition. *Alexandria Eng. J.* 64, 969–979. doi:10.1016/j.aej.2022.09.026

Rasheed, H. U., Khan, Z., El-Zahar, E. R., Shah, N. A., Islam, S., and Abbas, T. (2022). Homotopic solutions of an unsteady magnetohydrodynamic flow of Casson nanofluid flow by a vertical cylinder with Brownian and viscous dissipation effects. *Waves Random Complex Media* 0, 1–14. doi:10.1080/17455030.2022.2105979

Raza, A., Khan, U., Almusawa, M. Y., Hamali, W., and Galal, A. M. (2023). Prabhakar-fractional simulations for the exact solution of Casson-type fluid with experiencing the effects of magneto-hydrodynamics and sinusoidal thermal conditions. *Int. J. Mod. Phys. B* 37, 2350010. doi:10.1142/s0217979223500108

Raza, Q., Qureshi, M. Z. A., Khan, B. A., Kadhim Hussein, A., Ali, B., Shah, N. A., et al. (2022). Insight into dynamic of mono and hybrid nanofluids subject to binary chemical reaction, activation energy, and magnetic field through the porous surfaces. *Mathematics* 10, 3013. doi:10.3390/math10163013

Raza Shah Naqvi, S. M., Waqas, H., Yasmin, S., Liu, D., Muhammad, T., Eldin, S. M., et al. (2022). Numerical simulations of hybrid nanofluid flow with thermal radiation and entropy generation effects. *Case Stud. Therm. Eng.* 40, 102479. doi:10.1016/j.csite.2022.102479

Rizk, D., Ullah, A., Ikramullah,Elattar, S., Alharbi, K. A. M., Sohail, M., et al. (2022). Impact of the KKL correlation model on the activation of thermal energy for the hybrid nanofluid (GO+ZnO+Water) flow through permeable vertically rotating surface. *Energies* 15, 2872. doi:10.3390/en15082872

Sajid, M., Ali, N., Javed, T., and Abbas, Z. (2010). Stretching a curved surface in a viscous fluid. *Chin. Phys. Lett.* 27, 024703. doi:10.1088/0256-307x/27/2/024703

Sakkaravarthi, K., and Reddy, P. B. A. (2023). Entropy generation on Casson hybrid nanofluid over a curved stretching sheet with convective boundary condition: semi-analytical and numerical simulations. *Proc. Institution Mech. Eng. Part C J. Mech. Eng. Sci.* 237, 465–481. doi:10.1177/09544062221119055

Sarris, I. E., Lekakis, I., and Vlachos, N. S. (2002). Natural convection in a 2d enclosure with sinusoidal upper wall temperature. *Numer. Heat. Transf. Part A Appl.* 42, 513–530. doi:10.1080/10407780290059675

Shah, Z., Kumam, P., Ullah, A., Khan, S. N., and Selim, M. M. (2021). Mesoscopic simulation for magnetized nanofluid flow within a permeable 3D tank. *IEEE Access* 9, 135234–135244. doi:10.1109/access.2021.3115599

Shoaib, M., Kausar, M., Nisar, K. S., Asif Zahoor Raja, M., and Morsy, A. (2022). Impact of thermal energy on MHD casson fluid through a forchheimer porous medium with inclined non-linear surface: a soft computing approach. *Alexandria Eng. J.* 61, 12211–12228. doi:10.1016/j.aej.2022.06.014

Ullah, A., Ikramullah,Selim, M. M., Abdeljawad, T., Ayaz, M., Mlaiki, N., et al. (2021). A magnetite–water-based nanofluid three-dimensional thin film flow on an inclined rotating surface with non-linear thermal radiations and couple stress effects. *Energies* 14, 5531. doi:10.3390/en14175531

Ullah, I., Ullah, A., Selim, M. M., Khan, M. I., Saima,Khan, A. A., et al. (2022). Analytical investigation of magnetized 2D hybrid nanofluid (GO + ZnO + blood) flow through a perforated capillary. *Comput. Methods Biomechanics Biomed. Eng.* 25, 1531–1543. doi:10.1080/10255842.2021.2021194

Varun Kumar, R. S., Gunderi Dhananjaya, P., Naveen Kumar, R., Punith Gowda, R. J., and Prasannakumara, B. C. (2022). Modeling and theoretical investigation on Casson nanofluid flow over a curved stretching surface with the influence of magnetic field and chemical reaction. *Int. J. Comput. Methods Eng. Sci. Mech.* 23, 12–19. doi:10.1080/15502287.2021.1900451

Yogeesha, K. M., Megalamani, S. B., Gill, H. S., Umeshaiah, M., and Madhukesh, J. K. (2022). The physical impact of blowing, Soret and Dufour over an unsteady stretching surface immersed in a porous medium in the presence of ternary nanofluid. *Heat. Transf.* 51, 6961–6976. doi:10.1002/htj.22632

Zabihi, A., Akinshilo, A. T., Rezazadeh, H., Ansari, R., Sobamowo, M. G., and Tunc, C. (2022). Application of variation of parameter's method for hydrothermal analysis on MHD squeezing nanofluid flow in parallel plates. *Comput. Methods Differ. Equations* 10, 580–594. doi:10.22034/cmde.2021.41296.1794